Dalton Transactions

PAPER

View Article Online
View Journal | View Issue

Cite this: *Dalton Trans.*, 2016, **45**, 14591

Synthesis and catalytic applications of 1,2,3-triazolylidene gold(I) complexes in silver-free oxazoline syntheses and C–H bond activation†

René Pretorius,[a,b] Manuel R. Fructos,[c] Helge Müller-Bunz,[b] Robert A. Gossage,[a,d] Pedro J. Pérez*[c] and Martin Albrecht*[a,b]

Received 31st May 2016,
Accepted 23rd June 2016

DOI: 10.1039/c6dt02181f

www.rsc.org/dalton

A series of novel 1,2,3-triazolylidene gold(I) chloride complexes have been synthesised and fully characterised. Silver-free methodologies for chloride ion abstraction of these complexes were evaluated for their potential as Au-based catalyst precursors. Using simple potassium salts or MeOTf as chloride scavengers produced metal complexes that catalyse both the regioselective synthesis of oxazolines and the C–H activation of benzene or styrene for carbene transfer from ethyl diazoacetate. These results indicate that Ag-free activation of 1,2,3-triazolylidene gold(I) chloride complexes is feasible for the generation of catalytically active Au triazolylidene species. However, silver-mediated activation imparts substantially higher catalytic activity in oxazoline synthesis.

Introduction

Homogeneous catalysts comprised of gold as the active centre have enjoyed increased attention in recent years as more and more unique reactivity patterns have been revealed.[1] In particular, ligation by N-heterocyclic carbenes (NHCs) as for example in AuCl(IPr) (IPr = *N*,*N*′-bis(2,6-diisopropylphenyl)imidazolylidene) imparted exceptionally high catalytic activity,[1k,2] which spurred widespread efforts in this burgeoning area of catalysis. In comparison to classical, imidazole-derived NHCs, structurally related 1,2,3-triazolylidene (trz) ligands[3] have been significantly less studied as ligands in gold chemistry.[4] The triazole framework offers several benefits when compared with NHCs, including, for example, the ease of functional group incorporation,[3a,5] increased σ-donation compared to classical NHCs,[3,6] and a mesoionic resonance form which is able to potentially stabilise different metal oxidation states.[7] Catalytic activity in carbene gold complexes has typically been instigated by using a silver(I) salt as halide scavenger for catalyst activation.[8] However, Ag^+ can be a non-innocent activator in many Au-catalysed transformations, and often plays an active (and not always beneficial) role in the catalytic cycle.[1d,9] Current trends in Au catalysis are therefore focusing on using Ag-free protocols to avoid any undesired side-reactions. For example, pre-activation and subsequent silver salt removal from a stable cationic gold(I) complex as catalyst precursor has been described by Gagosz[10] Echavarren,[11] and others.[12] Also, the use of a gold(I) hydroxide[13] or acetate[14] pre-catalyst *in lieu* of gold(I) chloride complexes has also been shown to be an effective method to avoid the necessity of silver salts for catalyst activation. Several approaches towards Ag-free activation have been probed, though almost none are based on simple and inexpensive (commercial) salts. Thus, the *in situ* generation of active gold(I) catalysts has been explored by using Lewis acids as activators such as metal triflates,[15] and alkali metal salts of borates,[4a,16] to name a few.[17] However, with the exception of $Cu(OTf)_2$ (OTf = CF_3SO_3), the activators are typically non-commercial and customised salts.

We have recently demonstrated the non-innocent behaviour of silver(I) salts when activating 1,2,3-triazolylidene gold complexes.[18] Specifically, silver mediated carbene transfer reactions have been demonstrated, likely *via* a reverse carbene transfer from gold(I) to silver(I). Considering the significant complications arising from such ligand transfer, we

[a]*Department of Chemistry and Biochemistry, University of Bern, Freiestrasse 3, CH-3012 Bern, Switzerland. E-mail: perez@dqcm.uhu.es, martin.albrecht@dcb.unibe.ch*
[b]*School of Chemistry and Chemical Biology, University College Dublin, Belfield, Dublin 4, Ireland*
[c]*Laboratorio de Catálisis Homogénea, Unidad Asociada al CSIC, CIQSO-Centro de Investigación en Química Sostenible and Departamento de Química, Universidad de Huelva, Campus de El Carmen, 21007 Huelva, Spain*
[d]*Department of Chemistry & Biology, Ryerson University, 350 Victoria Street, Toronto, ON M5B 2K3, Canada*

† Electronic supplementary information (ESI) available: Synthesis of all novel triazoles and triazolium salts, NMR spectra of **2c**, tables of catalytic runs and crystallographic details. CCDC 1481151–1481154. For ESI and crystallographic data in CIF or other electronic format see DOI: 10.1039/c6dt02181f

endeavoured to establish alternative procedures for the activation of AuCl(trz) complexes for catalytic bond activation purposes, which do not rely on Ag^+ for chloride abstraction. Herein we demonstrate that simple potassium salts can be used to form catalytically active triazolylidene gold complexes. These methodologies are of further use for exploring the specific impact of triazolylidene ligands in gold(I)-mediated catalytic activity.

Results and discussion

Synthesis of triazolylidene gold complexes

A set of novel triazolylidene gold complexes AuCl(trz) were synthesised as representative examples intending to probe ligand induced catalytic effects. The ligand precursor triazolium salts **1a–e** (Scheme 1) were readily available through copper(I)-catalysed [2 + 3] dipolar cycloaddition reactions and subsequent alkylation with either $(Me_3O)BF_4$, MeI, or MeOTf ($OTf^- = SO_3CF_3^-$). Of note, triazolium **1b**, which contains a pendant acetate group was highly sensitive to hydrolysis and hence the alkylation of the triazole with MeOTf was performed at low temperature (below 0 °C). Subsequent storage of the triazolium salt **1b** below −20 °C is paramount to avoid spontaneous degradation over time. Salt **1c** was obtained in relatively low yields (about 30%) when compared to the other triazolium salts (≥79%), presumably because the electron withdrawing nature of the perfluorinated tail decreases the nucleophilicity of the triazole unit. The influence of the fluorocarbon unit is supported by the ^{1}H NMR chemical shifts for the NCH_2 signals, which are shifted downfield by 0.72 and 0.38 ppm, for N1 and N3 respectively, in comparison with the analogous protons of **1a**. Moreover, the *N*-bound methylene group appears in the ^{13}C NMR spectrum as a triplet ($^3J_{CF}$ = 21 Hz), indicating an interaction between the perfluorinated tail and the methylene group. In contrast, the ^{13}C NMR chemical shifts do not show any significant variation due to the more electron withdrawing nature of the fluoro-chain.

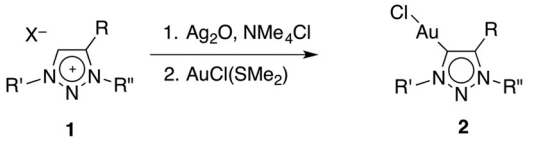

	R	R'	R"	X	yield of **2**
a	*n*Bu	*n*Bu	Me	BF_4	86%
b	CMe_2OAc	*n*Bu	Me	OTf	78%
c	*n*Bu	$(CH_2)_2C_6F_{13}$	$(CH_2)_2C_6F_{13}$	I	75%
d	Ph	adamantyl	Me	I	77%
e	Ph	2,6-(*i*Pr)$_2$C$_6$H$_3$	Me	OTf	64%
f	CMe_2OH	*n*Bu	Me	BF_4	88%

Scheme 1 Synthesis of triazolylidene gold(I) complexes **2**.

The AuCl(trz) complexes were synthesised from the triazolium salts **1a–f** using well established methodologies (Scheme 1).[4g,18,19] Accordingly, treatment of the appropriate triazolium salt with Ag_2O yielded the corresponding carbene silver intermediate, which was not isolated and used *in situ* for transmetallation with $AuCl(SMe_2)$. To ensure that chlorido complexes were formed exclusively, all novel AuCl(trz) complexes were prepared from triazolium salts containing either a BF_4^- or a OTf^- counterions, or alternatively by counterion exchange with $AgBF_4$ directly before the reaction with Ag_2O (for **1c**). Only traces of triazolylidene silver intermediate were formed in the absence of a chloride source according to ^{1}H NMR spectroscopic monitoring of the reaction, while clean and essentially quantitative formation of the intermediate was observed in the presence of Me_4NCl. The subsequent transmetalation was straightforward and good yields ranging from 64–88% were obtained for all gold complexes **2a–f** (see Experimental section).

Metallation of the hydroxyl-functionalised triazolium salt **1f** gave a mixture of products, with ratios that were dependent on the reaction conditions. In the presence of an excess Ag_2O and in moist solvents, complex **2f** was obtained in nearly 90% yield. Metallation of **1f** under an atmosphere of dry nitrogen and substoichiometric amounts of Ag_2O afforded significant amounts (up to 46%) of complexes **2g** and **2g′** as the major products (Scheme 2). We have not been able to separate these two products preparatively, though fractional crystallisation afforded single crystals of pure **2g** that were suitable for X-ray diffraction analysis (see below). Dissociation of the C-bound substituent in **2g** and **2g′** with formal loss of acetone was indicated by NMR spectroscopy. Two sets of resonances were observed, both featuring an additional resonance in the aromatic region and the disappearance of the two methyl groups of the wingtip unit of **1f**. Integration of the ^{1}H NMR resonances of the NCH_2 and NCH_3 signals suggest a 5 : 4 ratio of **2g** and **2g′**. The spectroscopic assignment was based on long range ^{1}H–^{13}C correlation spectroscopy (HMBC). Accordingly,

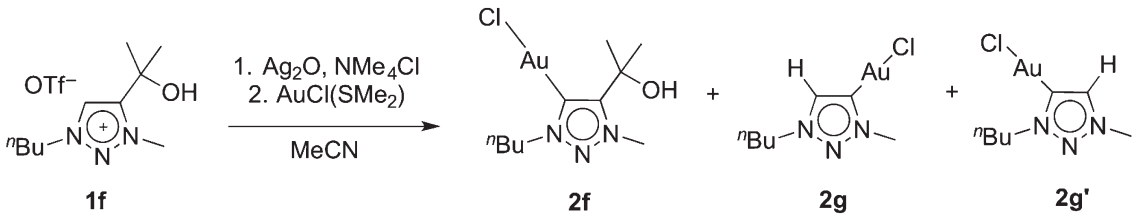

Scheme 2 Transmetallation of **1f** and concurrent partial formal loss of acetone resulting in the formation of **2f**, **2g**, and **2g′**.

the NCH_3 group of the C4-metallated complex **2g** resonantes at 4.20 ppm (*cf.* δ_H = 4.17 ppm in the C5-metallated homologue **2g′**), whereas the NCH_2 group in **2g′** appears at lower field than in **2g** (δ_H = 4.50 *vs.* 4.38 ppm) and provides the clearest spectroscopic distinction between the two isomers. The C_{trz}–H resonance shift is essentially identical in both complexes and appears at 7.58 and 7.57 ppm, respectively. Similarly, the ^{13}C NMR shifts of the two isomers are only marginally disparate. In agreement with the ^{1}H NMR data, the largest difference again pertains to the NCH_3 group (δ_C = 42.1 and 38.8) and the NCH_2 group (δ_C = 52.5 and 55.4 for **2g** and **2g′**, respectively). The resonances due to the $C_{trz}H$ carbons were significantly upfield shifted (δ_C = 134 ± 0.4) when compared to the normal 145–150 ppm range observed for C5-alkylated or -arylated triazolylidene gold complexes.

Formation of complexes **2g** and **2g′** may be rationalised by deprotonation of the hydroxyl group, which is followed by elimination of acetone from the ligand. The observation of isomers suggests that the ligand degraded before the triazolylidene silver intermediate is formed. Metallation of a C4,C5-diprotonated triazolium salt is unselective and may thus account for the formation of a mixture of **2g** and **2g′**. The influence of Ag_2O was therefore investigated in more detail. Using various **1f**/Ag_2O ratios (0.5, 1, 2) and monitoring of the triazolylidene silver complex formation indicated that higher equivalents of Ag_2O promoted the preservation of the wingtip group and hence promoted the formation of the silver intermediate that eventually leads to complex **2f**, while sub-stoichiometric quantities of Ag_2O increased substituent degradation. The isomeric ratio of the unsubstituted triazolylidene silver complexes is independent of the quantity of silver salt (*cf.* Table S1†), remains unchanged over time, and is in good agreement with the final product distribution observed for formation of complexes **2g** and **2g′**. These data therefore suggest that wingtip degradation of the ligand occurs prior to transmetallation and that acetone elimination is a competitive process to triazolium C_{trz}–H bond activation. Moreover, these results indicate that wingtip degradation only takes place from the triazolium salt, yet it is suppressed once the carbene silver precursor is formed. Otherwise, larger quantities of Ag_2O should shift the isomeric ratio due to degradation of the silver precursor of **2f**.

Characterisation of triazolylidene gold complexes

The ^{13}C NMR spectra of all triazolylidene gold complexes feature a resonance in the 156–162 ppm range for the Au-bound C_{trz} nucleus, consistent with related triazolylidene gold complexes.[4,18–20] The carbenic carbon is most deshielded in complex **2e** (δ_C = 162.1 ppm), and resonates at higher field in the alkyl-substituted triazolylidene complexes (δ_C = 157.5 ± 2.3 ppm) than in aryl-substituted triazolylidene complexes, suggesting that the electronic configuration of this carbon is affected by the triazolylidene substitution pattern. The polyfluorinated tail had no significant influence on the NMR frequency of the carbenic carbon. However, the NCH_2 group in complex **2c** is deshielded by 0.4 ppm (^{1}H NMR) when compared to the butyl homolog **2a**, and likewise shielded by about 8 ppm in the ^{13}C NMR spectrum.

Single crystal X-ray diffraction analysis of complexes **2b**, **2f**, and **2g** confirmed the bonding situation in these complexes and in particular demonstrated the wingtip dissociation in **2g** (Fig. 1). Bond lengths and angles of these complexes (Table 1) do not significantly deviate from related carbene gold complexes characterised previously.[4,18–20] However, some packing trends are worth noting. Complex **2g** displays a head-to-tail type packing, attributed to presumably weak aurophilic interactions (Au···Au separation of 3.46 Å) which may add to the electrostatic interaction between the chlorido ligand and the heterocyclic ring.[1f,21] This arrangement may be preferred due to the low steric demand of this ligand system, and hence allows for much closer packing than that of, for example, complex **2b**.

Catalysis results and activation studies

Previous work has clearly shown that Ag(I) can be a non-innocent activator for Au-catalysed transformations.[1d,9c,d,18,22] In particular when using AuCl(trz) system, silver has multiple roles beyond solely abstracting the gold-bound chlorido ligand and likely induces a retro-transmetallation to (transiently) yield catalytically active triazolylidene silver complexes.[9c,18,23]

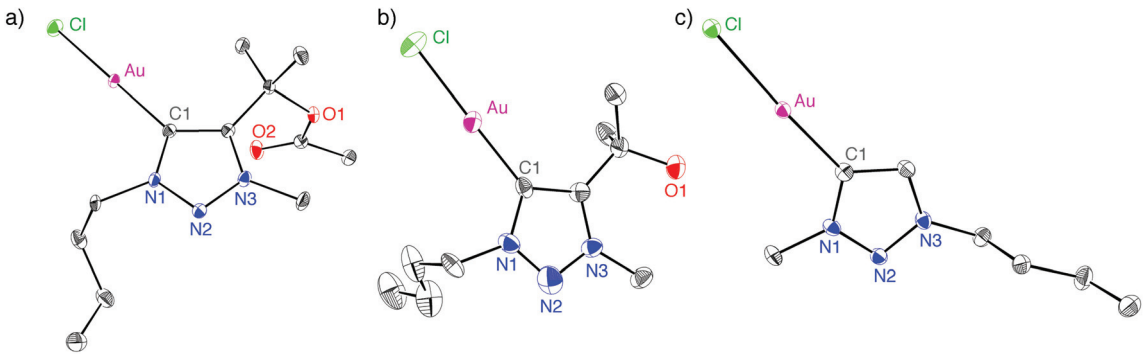

Fig. 1 ORTEP representations of complex **2b** (a), **2f** (b), and **2g** (c; all 50% probability ellipsoids, H-atoms and second independent molecule of **2g** in the unit cell omitted for clarity).

Table 1 Selected bond lengths [Å] and angles [°] in complexes **2b** and **2g**

Complex	Au–C1	Au–Cl	C1–Au–Cl
2b	1.995(2)	2.2896(6)	178.08(7)
2f	1.976(6)	2.2873(19)	178.1(2)
2g[a]	1.984(2)	2.2978(6)	175.90(7)

[a] Only for one of the two non-symmetry related molecules in the unit cell of **2g**.

Because of these complications and the associated uncertainty whether the true catalytic species is (are) based on silver or gold, silver-free catalyst activation methodologies are of paramount importance.[16] We considered two specific routes: (i) halide abstraction with a potassium salt, and (ii) the use of CH_3^+ as an electrophile. Even though methyl cations are only rarely used to scavenge chloride, chloride to halide exchange reactions at the metal centre have been performed successfully with methyl iodide.[24] Moreover, C–C bond formation by electrophilic activation of (NHC)Au(Aryl) complexes has been reported.[25] To probe this methodology, complex **2a** was reacted with stoichiometric equivalents of MeOTf in MeCN. Initial attempts to isolate the putative cationic solvent complex [(trz)Au(solv)]OTf from the reaction mixture only afforded Au(0), indicated by the gold mirror that formed upon evaporation of all volatiles. Monitoring the reaction by ^{19}F NMR spectroscopy (CD_2Cl_2) indicated a new resonance that is shifted 5 ppm upfield from MeOTf, attributed to the gradual formation of a new ion pair in solution (see ESI, Fig. S1†). The corresponding ^{1}H NMR data showed only minor changes in the ligand, and a new resonance around 3 ppm which has been assigned to CH_3Cl. In order to overcome the apparent instability of the cationic species resulting from **2a**, it was trapped by the addition of an exogenous ligand. Addition of isonitrile (methyl isocyanoacetate) gave the corresponding cationic complex (see ESI†).[18] Likewise, addition of PPh_3 before evaporation of the solvent afforded the cationic gold species **3a**. This complex was unambiguously identified by NMR spectroscopy and X-ray diffraction (Fig. 2). However, it should be noted that the phosphine carbene gold complex cation is also formed upon treatment of **2a** with PPh_3 in the absence of any electrophilic chloride scavenger (albeit with a chloride counterion), which limits the relevance of phosphines as trapping reactions. In contrast, isonitrile binding does not occur with the [AuCl(trz)] complexes **2** spontaneously and was only observed in the presence of MeOTf, suggesting that isonitriles are more diagnostic trapping agents.

Analysis of complex **3a** by ^{13}C and ^{31}P NMR spectroscopy reveals similar features when compared to related $[(trz)Au(PPh_3)]^+$ and $[(NHC)Au(PPh_3)]^+$ complexes (*e.g.* δ_P = 39.4 for **3a**).[18,26] The carbenic nucleus is deshielded by about 15 ppm compared to the chlorido analogue **2a** and appears at δ_C = 172, in agreement with a more electron-deficient metal fragment. X-ray diffraction analysis of single crystals of **3a** indicates an elongation of the gold carbene distance compared to **2a** (Au–C1 2.046(3) Å in **3a** *vs.* 1.98 Å in complexes **2**), a consequence of the higher *trans* influence of PPh_3 compared to the chlorido ligand. The coordination geometry slightly deviates from linearity, P–Au–C1 172.57(9)°, presumably due to packing constraints. Alternating layers of triflate ions and triazolium units with close contacts of 3.13 and 3.53 Å suggest electrostatic interactions in the solid state between the formally negatively charged triflate oxygen sites and the partially positively charged heterocycle.

Catalytic activity in oxazoline synthesis

Halide abstraction under catalytically relevant conditions was probed in the presence of isonitriles and bromobenzaldehyde to promote the catalytic formation of oxazolines.[12d–g,18,27] Complex **2a** was chosen as a representative AuCl(trz) complex because of the simple ligand design and the established benefit of the triazolylidene substitution pattern for monitoring catalytic reactions.[7d] Activation of this complex for initiating catalytic activity was investigated using MeOTf as well as different potassium salts (Table 2).

A systematic variation of the different reaction parameters revealed that the gold complex, amine, and a chloride scavenger are needed for generating an active species (entries 1–5).[28] Comparison of different chloride scavenging additives revealed that KPF_6 (entry 5) is superior to other potassium salts (entries 6 and 7). The addition of N^iPr_2Et is essential for catalytic turnover, as no catalytic activity was observed in the absence of base (entry 4).[18] Likewise the reaction is very slow when no scavenger was used (entry 3). Interestingly, KBF_4 has no activating effect (*cf.* entries 3 and 6). The utilisation of MeOTf enhanced

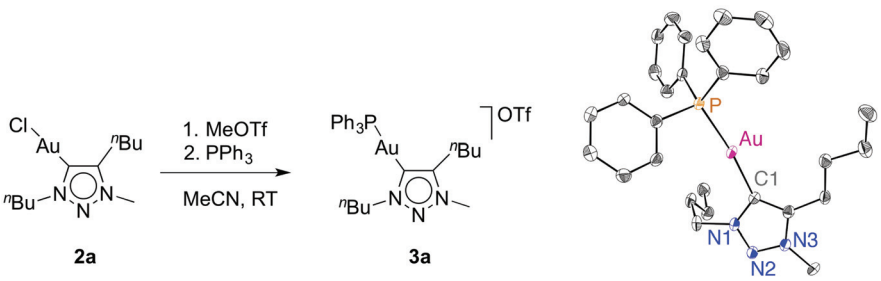

Fig. 2 Synthesis and ORTEP representation of complex **3a** (50% probability, hydrogens and OTf^- anion omitted for clarity); Au1–C1 2.046(3) Å, Au1–P1 2.2817(8), Cl1–Au–P1 172.57(9)°.

Table 2 Catalytic oxazolines synthesis with various AuCl(trz) complexes and activators[a]

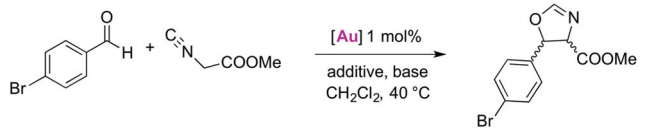

Entry	[Au]	Additive	Base	Conversion (%)	*cis*/*trans*
1	—	—	—	6	—
2	—	KPF_6	N^iPr_2Et	25	—
3	**2a**	—	N^iPr_2Et	24	23/77
4	**2a**	KPF_6	—	<2	—
5	**2a**	KPF_6	N^iPr_2Et	93	26/74
6	**2a**	KBF_4	N^iPr_2Et	21	18/82
7	**2a**	KOTf	N^iPr_2Et	61	28/72
8	**2a**	MeOTf	N^iPr_2Et	62	27/73
9	**2b**	KPF_6	N^iPr_2Et	88	27/73
10	**2c**	KPF_6	N^iPr_2Et	75	29/71
11	**2d**	KPF_6	N^iPr_2Et	87	29/71

[a] General conditions: 4-bromobenzylaldehyde (1.6 mmol), methyl isocyanoacetate (1.4 mmol), N^iPr_2Et (0.14 mmol), AuCl(trz) (0.014 mmol), additive (0.028 mmol), trimethoxybenzene (0.36 mmol, internal standard), CH_2Cl_2 (4 mL), 40 °C, 8 h; yields and *cis*/*trans* ratio determined by ^1H NMR spectroscopy, averaged of at least 2 runs.

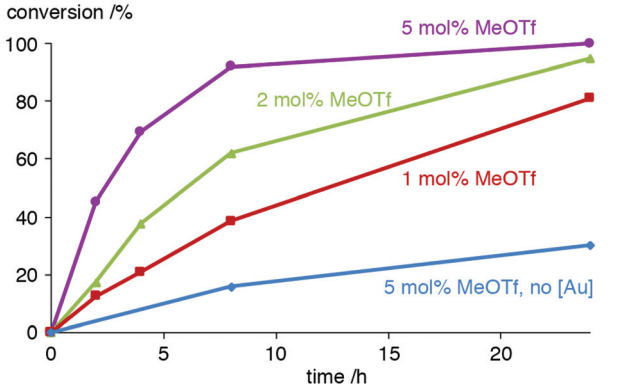

Fig. 3 Comparison of the conversion for catalytic oxazoline synthesis using **2a** in combination with varying amounts of MeOTf (red, green, and purple traces), and using MeOTf in the absence of a gold complex (blue trace).

catalytic activity (entry 8), suggesting that chloride methylation is a viable strategy to generate the labile coordination site at the gold centre. It is remarkable that KOTf and MeOTf result in the same catalytic activity (entries 7 and 8) and give identical conversions, suggesting a distinct role for the OTf^- anion in levelling catalyst activity.[1e] Tentatively, weak triflate coordination may be surmised to slow down the turnover frequency when compared to the analogous species containing a PF_6^- counterion. The relevance of the counterion is also indicated by the variable catalytic activity in dependence of different anions in the potassium salts (entries 5–7).

Further studies on using MeOTf to activate the AuCl(trz) catalyst precursor included the variation of the equivalents of this activator, a modification which affected the conversion rates markedly. Using only 1.1 instead of 2 equiv. MeOTf with respect to **2a** reduced the activity to about half (*e.g.* 21% *vs.* 38% conversion after 4 h, Fig. 3 and Table S2†). In the presence of 5 equiv. MeOTf, the catalytic activity is doubled and almost full conversion was accomplished after 8 h (45% already after 2 h), which matches the conversion rates achieved upon activation of the gold complex with KPF_6. The need for higher relative ratios of additive may be because MeOTf may interact with N^iPr_2Et or undergo partial hydrolysis.

The enhancement of catalytic activity in the presence of KOTf, MeOTf and in particular KPF_6 suggests the successful formation of a $[(trz)Au]^+$ species for substrate conversion. Therefore, KPF_6, was utilised as activator for a catalytic screening of the AuCl(trz) complexes **2a–d** (entries 5, 9–11). In this series, the catalytic activity of **2a**, **2b**, and **2d** is identical within the measurement errors (±5%). Complex **2c** containing perfluorinated substituents on the triazolylidene induced slightly lower catalytic activity. This effect is particularly pronounced at early conversion stages. Thus after 2 h and 4 h, runs with complex **2c** achieved 25% and 43% conversion, respectively, while the other complexes are considerably more active (average 38% and 65% conversion after the same reaction time). The lower performance of complex **2c** may be associated with the specific solubility and aggregation properties imparted by the perfluorinated substituents. Variation of the hydrocarbon substituents on the triazolylidene ligand from linear or branched alkyl groups to aryl substituents does not affect the catalytic performance (*cf.* **2a** *vs.* **2b** and **2d**). These results therefore suggest that the catalytic rate-determining step is not significantly governed by steric or electronic effects induced by the triazolylidene ligand. This conclusion is further supported by the essentially unaltered *cis*/*trans* ratio, even when a sterically demanding adamantyl group was included in the ligand scaffold (**2d**, entry 11).

Importantly, activation of complex **2a** with $AgBF_4$ affords a species that is two to three orders of magnitude more active than the species generated with KPF_6 or triflates, reaching quantitative oxazoline formation within 15 min at 0.5 mol% loading.[18] Similarly high activities have been recorded when related triazolylidene silver complexes (trz)AgCl were used for catalysis in the absence of gold.[29] Thus, the gold-based active species are considerably less competitive than their triazolylidene silver analogues in this catalytic heterocycle synthesis. These data further suggest that the catalytically active component in the AuCl(trz)/$AgBF_4$ system may be a $[(trz)Ag]^+$ species resulting from a retro-transmetallation or the formation of Au nanoparticles.[15a,18,29]

C–H bond activation in metal-mediated carbene transfer from ethyl diazoacetate

The application of Ag-free $[(trz)Au]^+$ catalysis was further probed in carbene transfer chemistry by the metal-mediated decomposition of diazo compounds. This catalytic system is attractive for several reasons. Firstly, $NaBAr^F{}_4$ ($BAr^F{}_4$ = tetrakis(3,5-bis(trifluoromethyl)phenyl)borate) has been shown to be

an excellent activator for AuCl(NHC) catalysts in this area of catalysis and hence allows for Ag-free activation.[30] In particular the AuCl(IPr)/$NaBAr^F_4$ system has given promising results with arenes as substrates. With previously described catalytic systems,[31] the reaction of benzene and ethyl diazoacetate (EDA) led to cycloheptatriene (**4** in Table 3), as the result of consecutive double bond cyclopropanation and ring expansion in the so-called Buchner reaction. However, the gold-based system is selective towards C–H bond functionalisation of benzene and other arenes by formal carbene insertion affording an alkyl-arene (**5** in Table 3).[30a–c] Furthermore, it was shown that AuCl(trz)/$AgSbF_6$ systems are useful carbene transfer reagents from EDA to both reactive *N*- or *O*-containing substrates.[4g] Since the activity of the AuCl(trz) systems for C–H insertion has not been studied, the catalytic C–H activation with EDA seems an attractive expansion to investigate Ag-free activation of AuCl(trz). Benzene was chosen as a representative substrate for preliminary screening, and the activity of complexes **2a–2e** in catalytic carbene transfer was monitored using $NaBAr^F_4$ as additive (Table 3). While a mixture of the aforementioned cycloheptatriene **4** and benzyl acetate **5** is expected, these two products are easily distinguishable by their diagnostic NMR signals.

All AuCl(trz) complexes **2a–e** favoured the formation of the cycloheptatriene product **4** over the product from C–H insertion in approximately a 3 : 1 ratio (Table 3, entries 1–5). The catalytic activity is essentially insensitive to the substitution pattern on the triazolylidene heterocycle with overall product ratios, *i.e.* **4** + **5**, all in the 75–85% range. The influence of silver salts as halide scavengers was also considered to determine potential interactions of silver in the catalytic cycle (entries 6–8). While the use of $AgBF_4$ further promoted cyclopropanation and yielded a 8 : 1 selectivity towards **4** (entry 6), $AgSbF_6$ did not alter the product distribution when compared to the activation of AuCl(trz) with $NaBAr^F_4$ (entries 7 and 8). We also noted that the consumption of EDA was not complete (*ca.* 85%, see Table 3) even after 24 h. Furthermore, the species generated from AuCl(trz) and $NaBAr^F_4$ in CH_2Cl_2 was unstable in the absence of coordinating substrates as displayed by the immediate formation of gold(0) and gold nanoparticles observed as purple particles in solution. This instability required addition of EDA before introducing the additive for generating the active catalyst. This sequence of addition resulted in the formation of fumarate and maleate as minor by-products. Such side-product formation is typically suppressed by slow addition of EDA,[32] though this procedure is prohibited here because of the instability of the $[Au(trz)]^+/BAr^F_4$ species.

Similar reactivity patterns were observed when using selected AuCl(trz) complexes for carbene transfer to styrene (Table 4). These runs were performed in CH_2Cl_2 solution, in contrast to the neat benzene catalysis. The results indicate that the active species is solvent tolerant and apparently does not react with CH_2Cl_2 but instead selectively activates the aromatic C–H bonds. As in the case of benzene, full conversion of EDA was not achieved within 24 h and about 10% EDA remained unconverted after that time, which resulted in a complex reaction mixture for NMR analysis. Nonetheless, the ratio of products confirmed the same trend noted for diazocarbene transfer to benzene. Thus, carbene addition to a C=C double bond and formation of the phenyl cyclopropane **6** is the major outcome of the reaction, while carbene insertion into a C_{aryl}–H bond and formation of styryl acetate **7** is less favoured. The ratio between cyclopropanation and C–H bond activation is about 3 : 1 for complexes **2b,d,e** and hence very similar to the ratios obtained when using benzene as substrate (entries 2–4).

Table 3 Triazolylidene gold-mediated carbene transfer from EDA to benzene[a]

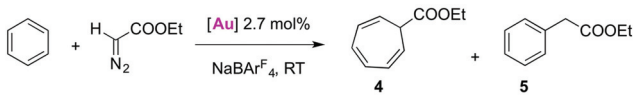

			Product ratio[b]		
Entry	[Au]	Additive	**4**	**5**	DEF/DEM[c]
1	**2a**	$NaBAr^F_4$	68	17	15
2	**2b**	$NaBAr^F_4$	65	18	17
3	**2c**	$NaBAr^F_4$	61	19	21
4	**2d**	$NaBAr^F_4$	57	17	26
5	**2e**	$NaBAr^F_4$	67	16	17
6	**2a**	$AgBF_4$	77	9	14
7	**2a**	$AgSbF_6$	64	18	18
8	**2e**	$AgSbF_6$	62	22	16

[a] General conditions: [Au] (0.012 mmol), benzene (3 mL), EDA (0.44 mmol), $NaBAr^F_4$ (0.015 mmol), ratios in % of product mixture. [b] Distribution of products according to ^{1}H NMR spectroscopy, *ca.* 15% of EDA were remaining after 24 h as quantified with benzaldehyde as internal standard. [c] DEF/DEM: diethyl fumarate/diethyl maleate, by products of the carbene coupling reaction from two molecules of EDA.

Table 4 Triazolylidene gold-mediated carbene transfer from EDA to styrene[a]

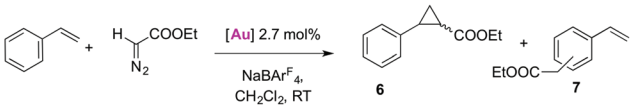

			Product ratio[b]		
Entry	[Au]	Additive	**6**	**7**	DEF/DEM[c]
1	**2a**	$NaBAr^F_4$	77	12	11
2	**2b**[b]	$NaBAr^F_4$	65	20	15
3	**2d**	$NaBAr^F_4$	59	17	24
4	**2e**	$NaBAr^F_4$	66	21	13
5	**2a**	$AgSbF_6$	74	13	12
6	**2d**	$NaBAr^F_4$, Hg drop	67	20	13

[a] General conditions: [Au] (0.012 mmol), styrene (2.3 mmol), EDA (0.44 mmol), $NaBAr^F_4$ (0.015 mmol), CH_2Cl_2 (2 mL); average of 2 runs. [b] Distribution of products according to ^{1}H NMR spectroscopy, *ca.* 10% of EDA were remaining after 24 h as quantified with benzaldehyde as internal standard. [c] DEF/DEM: diethyl fumarate/diethyl maleate, by products of the carbene coupling reaction from two molecules of EDA.

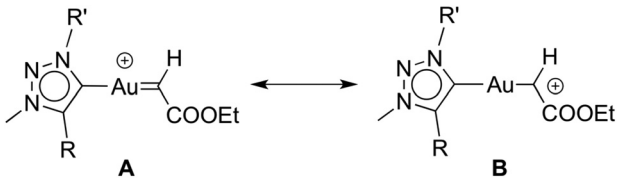

Scheme 3 Resonance forms for the gold–carbene intermediate.

In contrast, complex **2a** is considerably more selective and reaches a 6.5 : 1 product ratio (entry 1).

No significant change in activity or selectivity was observed upon substituting the chloride scavenger from $NaBAr^F_4$ to a silver salt (entry 5). The similar performance suggests that unlike in the oxazoline syntheses (*vide supra*), the catalytically active species in the carbene transfer reaction remains the $[(trz)Au]^+$ species. Finally, a Hg-drop test was performed using catalyst **2d**. No significant deviation was noted when compared to the parent run (*cf.* entries 3 and 6), which is indicative of a homogeneous catalytic cycle rather than one involving nanoparticles as an active species.

It is worthwhile to compare complexes AuCl(trz) and AuCl(IPr) as catalyst precursors to give some insight into the ligand effects. Firstly, the activity of the $[(trz)Au]^+$ species is substantially lower than that of $[(IPr)Au]^+$, requiring more than 24 h rather than just 6 h to reach complete conversion under identical conditions.[30c] Secondly, and perhaps more importantly, the active species resulting from AuCl(trz) strongly favours cyclopropanation over C–H bond activation and carbene insertion, while the use of AuCl(IPr) favours C–H bond activation. However, the product ratio for the AuCl(trz) systems closely matches those found for functionalised AuCl(NHC) systems.[30d] As the reactivity pattern was essentially identical for all the evaluated triazolylidene complexes, this facet likely reflects the different properties induced by triazolylidenes *vs.* classical NHC ligands. Previous work has suggested that decreasing electron density on the metal centre favours C–H insertion. In agreement with such a model, the increased σ-donor properties of mesoionic triazolylidenes indeed results in preferential cyclopropanation as compared to carbene insertion *via* C–H activation.[30a,33] Accordingly, an increased electron density at the metal centre favours a carbene type resonance structure for the diazo fragment (**A**, Scheme 3) while electron-poorer metal centres induce a carbocationic structure (**B**, Scheme 3).[34] It is very likely that the relative weight of each limiting structure in the real structure influences the reaction outcome toward the addition (Buchner) or insertion (alkyl-carbene) products.

Conclusions

A range of Ag-free chloride scavenger reagents for application with triazolylidene gold(I) complexes has been tested and shown to be useful for the activation of these complexes prior to catalysis. The results indicate that the Au complexes are less active catalysts for oxazoline synthesis than the analogous silver complexes such as AgCl(trz).[29] Also, due to the linear coordination sphere around the metal centre, variation of the ligand substituents only moderately modulated catalytic activity and did not alter the diastereoselectivity of the resulting product profile. The AuCl(trz)/$NaBAr^F_4$ system also catalysed the carbene transfer from EDA *via* benzene and styrene C–H bond activation. This activity demonstrated further applications of Ag-free $[(trz)Au]^+$ catalysis. In this case, cyclopropanation products were favoured over C–H insertions, in contrast to the AuCl(IPr) system, indicating that the strong σ-donor properties of triazolylidene can be used to modulate the selectivity of gold in catalytic processes. Considering these results in combination with previous studies, it can be concluded that the choice of chloride scavenger is important to effectively identify the activity of gold-based catalysts and to assess the impact of the metal, as well as that of the ligand framework.

Experimental

General

The precursor 4-butyl-1-(3,3,4,4,5,5,6,6,7,7,8,8,8-tridecafluorooctyl)-1*H*-1,2,3-triazole for the triazolium salts **1c**,[35] the triazolium salts **1a**,[36] and **1e**,[3d] and the triazolylidene gold complex **2d** were synthesised using literature procedures.[18] The synthesis of all novel triazoles and triazolium salts is described in the ESI.† Ag_2O was used after regeneration by heating >160 °C under vacuum. Dry, degassed solvents were purified using an alumina/catalyst column (Thermovac Co.). All other reagents are commercially available and were used as received. All microwave experiments were carried out using a Biotage Initiator 2.5 instrument, operating at 0–400 W irradiation power. Unless specified otherwise NMR were recorded at 25 °C, on Varian and Bruker spectrometers operating at 300, 400, or 500 MHz (^{1}H NMR) and 75, 100, 125 MHz ($^{13}C\{^1H\}$ NMR) respectively. Chemical shifts (δ in ppm, coupling constants J in Hz) were referenced to residual solvents. Assignments are based on homo- and heteronuclear shift correlation spectroscopy. Elemental analyses were performed by the Microanalytical Laboratory at University College Dublin, Ireland using an Exeter Analytical CE-440 Elemental Analyzer, with the exception of complex **2d** which was performed in Unidad de Análisis Elemental of the Universidad de Huelva. Residual solvents were identified by NMR spectroscopy GC analysis were recorded on a Varian CP-3800 instrument. High-resolution mass spectrometry was carried out with a Micromass/Waters Corp. USA liquid chromatography time-of-flight spectrometer equipped with an electrospray source.

Complex 2a. To a solution of **1a** (290 mg, 1.0 mmol) in dry CH_2Cl_2/MeCN (20 mL, 1 : 1 v/v) were added Ag_2O (134 mg, 0.58 mmol), and NMe_4Cl (140 mg, 1.3 mmol), and the suspension was stirred for 16 h under the exclusion of light under a N_2 atmosphere. AuCl(SMe_2) (309 mg, 1.1 mmol) was added and stirring continued for 2 h. The reaction mixture was filtered through Celite and volatiles were removed under reduced pressure. The residue was redissolved in CH_2Cl_2 and filtered

through Celite a second time to remove residual salts. Volatiles were removed under reduced pressure yielding the product as a brown oil, which became crystalline after several days of drying *in vacuo* (0.376 g, 0.88 mmol, 86%). ^{1}H NMR (500 MHz, $CDCl_3$): δ 0.95 (m, 6H, 2 × CH_2CH_3), 1.32–1.44 (m, 4H, 2 × 2 CH_2CH_3), 1.68–1.74 (m, 2H, $C_{trz}CH_2CH_2$), 1.98–2.04 (m, 2H, NCH_2CH_2), 2.76 (t, $^3J_{HH}$ = 7.8 Hz, 2H, $C_{trz}CH_2$), 4.02 (s, 3H, NCH_3), 4.42 (t, J_{HH} = 7.3 Hz, 2H, NCH_2) $^{13}C\{^1H\}$ (126 MHz, $CDCl_3$): δ 13.4 ($NCH_2CH_2CH_2CH_3$), 13.9 ($C_{trz}CH_2CH_2CH_2CH_3$), 19.8 ($NCH_2CH_2CH_2$), 22.5 ($C_{trz}CH_2CH_2CH_2$), 24.9 ($C_{trz}CH_2$), 31.4 ($C_{trz}CH_2CH_2$), 32.3 (NCH_2CH_2), 36.4 (NCH_3), 55.1 (NCH_2), 147.5 ($C_{trz}CH_2$), 157.0 (C_{trz}–Au) HRMS (ESI+): *m*/*z* Found 450.0987 $[M + Na]^+$ (calcd for $C_{11}H_{21}N_3AuClNa$, 450.1028) Anal. Calcd for $C_{11}H_{21}N_3AuCl$: C, 30.89; H, 4.97; N, 9.82%. Found: C, 31.04; H, 4.72; N, 9.69%.

Complex 2b. This complex was prepared according to the procedure described for **2a** starting from triazolium salt **1b** (200 mg, 0.51 mmol), Ag_2O (60 mg, 0.26 mmol), NMe_4Cl (60 mg, 0.55 mmol), and $AuCl(SMe_2)$ (156 mg, 0.53 mmol). After filtration through Celite and concentration under reduced pressure, pentane was added. The formed black coloured solids were removed by filtration and the supernatant evaporated to dryness. The residue was repeatedly dissolved in CH_2Cl_2 and precipitated with Et_2O until a minor amount of white precipitate was observed. The supernatant was then decanted, evaporated to dryness, washed with pentane, and dried *in vacuo*. This procedure yielded complex **2b** as a white solid (0.19 g, 0.40 mmol, 78%). Crystals were obtained by slow diffusion of Et_2O into a CH_2Cl_2 solution. ^{1}H NMR (500 MHz, $CDCl_3$): δ 0.96 (t, $^3J_{HH}$ = 7.4 Hz, 3H, CH_2CH_3), 1.33–1.40 (m, 2H, CH_2CH_3), 2.04–2.07 (m, 8H, NCH_2CH_2 and $C(CH_3)_2$), 2.10 (s, 3H, C═OCH_3), 4.14 (s, 3H, NCH_3), 4.49 (t, $^3J_{HH}$ = 7.1 Hz, 2H, NCH_2) $^{13}C\{^1H\}$ (126 MHz, $CDCl_3$): δ 13.6 (CH_2CH_3), 19.8 (CH_2CH_3), 22.0 (C═OCH_3), 29.1 ($C(CH_3)_2$), 32.3 (NCH_2CH_2), 39.6 (NCH_3), 56.1 (NCH_2), 76.7 (CC_{trz}), 149.4 (CC_{trz}), 156.6 (C_{trz}–Au), 169.5 (C═O) HRMS (ESI+): *m*/*z* Found 494.0886 $[M + Na^+]$ (calcd for $C_{12}H_{21}N_3O_2ClAuNa$, 494.0886) Anal. Calc. for $C_{12}H_{21}N_3AuClO_2$: C, 30.55; H, 4.49; N, 8.91%. Found: C, 30.28; H, 4.31; N, 8.63%.

Complex 2c. $AgBF_4$ (41 mg, 0.21 mmol) was added to a solution of **1c** (0.18 g, 0.19 mmol) in dry CH_2Cl_2/MeCN (30 mL, 1 : 1 v/v), an stirred with the exclusion of light under a N_2 atmosphere for 5 min. This mixture was treated with Ag_2O (27 mg, 0.12 mmol) and NMe_4Cl (26 mg, 0.24 mmol) and the reaction was stirred for 16 h in the dark. Then $AuCl(SMe_2)$ (56 mg, 0.19 mmol) was added and the reaction stirred for a further 2 h. The reaction mixture was exposed to air and the product was purified as described for **2a** by repeated filtering through Celite, affording complex **2c** as a pale yellow solid (150 mg, 0.14 mmol, 75%). ^{1}H (500 MHz, $CDCl_3$): δ 0.97 (t, $^3J_{HH}$ = 7.3 Hz, 3H, CH_2CH_3), 1.39–1.47 (m, 2H, CH_2CH_3), 1.73–1.79 (m, 2H, CCH_2CH_2), 2.8–3.01 (m, CCH_2, 6H, 2 × NCH_2CH_2), 4.62 (t, $^3J_{HH}$ = 7.1 Hz, 2H, N3CH_2), 4.82 (t, $^3J_{HH}$ = 6.8 Hz, 2H, N1CH_2) $^{13}C\{^1H\}$(126 MHz, $CDCl_3$): δ 13.8 (CH_2CH_3), 22.4 (CH_2CH_3), 24.9 ($C_{trz}CH_2$), 30.9 (t, $^3J_{CF}$ = 22.2 Hz, N3CH_2CH_2), 31.3 (t, $^3J_{CF}$ = 20.1 Hz, N1CH_2CH_2), 31.6 ($C_{trz}CH_2CH_2$), 42.2 (N3CH_2), 47.7 (N1CH_2), 146.7 ($C_{trz}CH_2$), 158.5 (C_{trz}–Au) $^{19}F\{^1H\}$(470 MHz, $CDCl_3$): δ −126.27–(−126.12) (m, 4F), −123.4, −123.2 (2 × br, 2 × 2F), −122.9 (br, 4F), −121.97–(−121.79), −114.23–(−14.05) (2 × m, 2 × 4F), −80.88–(−80.80) (m, 6F) Anal. Calcd for $C_{22}H_{17}AuClF_{26}N_3$: C, 25.17; H, 1.63; N, 4.00%. Found: C, 25.18: H, 1.30; N, 3.80%.

Complex 2e. Triazolium salt **1e** (87 mg, 0.9 mmol), Ag_2O (29.8 mg, 0.13 mmol), and NMe_4Cl (20.1 mg, 0.18 mmol) were stirred in dry CH_2Cl_2/MeCN (10 mL, 1 : 1 v/v) under a N_2 atmosphere, for 17 h with the exclusion of light. Volatiles were removed *in vacuo*, and the residue was suspended in dry CH_2Cl_2 (15 mL), and stirred with $AuCl(SMe_2)$ (54.9 mg, 0.19 mmol) in the dark for 2 h. The reaction mixture was filtered through Celite, eluted with CH_2Cl_2 and all volatiles were removed. The product was obtained as a white solid (65 mg, 0.12 mmol, 64% yield). Crystals were obtained by slow diffusion of dry Et_2O into a CH_2Cl_2 solution at −20 °C. ^{1}H (500 MHz, $CDCl_3$): δ 1.14 (d, $^3J_{HH}$ = 6.9 Hz, 6H, $CH(CH_3)_2$), 1.34 (d, $^3J_{HH}$ = 6.9 Hz, 6H, $CH(CH_3)_2$), 2.31 (sept, $^3J_{HH}$ = 6.9 Hz, 2H, 2 × $CH(CH_3)_2$), 4.25 (s, 3H, NCH_3), 7.31 (d, $^3J_{HH}$ = 7.8 Hz, 2H, $C_{DiIPr}H$), 7.53–7.58 (m, 4H, $C_{Ar}H$), 7.80–7.82 (m, 2H, $C_{Ar}H$) $^{13}C\{^1H\}$(126 MHz, $CDCl_3$): δ 24.2, 24.5 (2 × $CHCH_3$), 28.9 ($C_{DiIPr}H$), 38.4 (NCH_3), 124.4 ($C_{Ar}H$), 126.0 (C_{Ph}), 129.4, 129.8, 130.7 (3 × $C_{Ph}H$), 131.6 ($C_{Ar}H$), 135.2, 145.2 (2 × C_{Ar}), 146.8 ($C_{trz}C$), 162.1 (C_{trz}–Au) Anal. Calcd for $C_{21}H_{25}AuClN_3{\cdot}\frac{1}{2}CH_2Cl_2$: C, 43.45; H, 4.41; N, 7.07%. Found: C, 43.28; H, 4.50; N, 6.79%.

Complex 2f. The triazolium tetrafluoroborate **1f** (77.5 mg, 0.27 mmol), NMe_4Cl (29 mg, 0.26 mmol), and Ag_2O (31.9 mg, 0.14 mmol) were stirred in CH_2Cl_2/MeCN (5 mL, 1 : 1 v/v) for 16 h protected from light. To this mixture was added AuCl (SMe_2) (79.5 mg, 0.27 mmol) and stirring was continued for 2 h. The suspension was filtered through Celite, eluted with CH_2Cl_2 and the volatiles were removed under reduced pressure yielding the crude product as an off-white solid (98 mg 23 mmol, 88%). Crystals were grown by slow evaporation of a CH_2Cl_2/Et_2O solution of **2f**. ^{1}H (400 MHz, CD_2Cl_2): δ 0.97 (t, $^3J_{HH}$ = 7.4 Hz, 3H, CH_2CH_3), 1.33–1.43 (m, 2H, CH_2CH_3), 1.89 (s, 6H, $C(CH_3)_2$), 1.99–2.06 (m, 2H, NCH_2CH_2), 4.29 (s, 3H, NCH_3), 4.47 (t, $^3J_{HH}$ = 7.3 Hz) $^{13}C\{^1H\}$(101 MHz, CD_2Cl_2): δ 13.8 (CH_2CH_3), 21.2 (CH_2CH_3), 32.6, 32.7 (NCH_2CH_2 and $C(CH_3)_2$), 41.0 (NCH_3), 56.2 (NCH_2), 151.7 ($C_{trz}C$), 155.2 (C_{trz}–Au).

Complex 2g and 2g′. A suspension of the triazolium tetrafluoroborate **1f** (100 mg, 0.35 mmol), Ag_2O (80 mg, 0.35 mmol), NMe_4Cl (80 mg, 0.73 mmol), and activated molecular sieves in dry CH_2Cl_2 (25 mL) was stirred under the exclusion of light for 3 days, under a N_2 atmosphere. $AuCl(SMe_2)$ (103 mg, 0.35 mmol) was added and the reaction stirred for 2 h. The reaction mixture was then filtered through Celite, and all volatiles were removed under reduced pressure, which yielded **2g** as a pale yellow solid (37 mg, 0.10 mmol, 28% yield). Crystals were grown by slow evaporation of CH_2Cl_2. The same result was obtained when the reaction was started from the triazolium triflate analogue of **1f**. ^{1}H (400 MHz, $CDCl_3$): δ 0.94–1.01 (m, 3H, CH_2CH_3), 1.32–1.44 (m, 2H, CH_2CH_3), 1.89–1.98 (m, 2H, NCH_2CH_2), 4.20 (s, 3H, NCH_3), 4.38

(t, $^3J_{HH}$ = 7.3 Hz, 2H, NCH_2), 7.57 (s, 1H, $C_{trz}H$) $^{13}C\{^1H\}$(101 MHz, $CDCl_3$): δ 13.4 or 13.6 (CH_2CH_3), 19.7 (CH_2CH_2), 31.6 (NCH_2CH_2), 42.1 (NCH_3), 52.5 (NCH_2), 133.6 ($C_{trz}H$), 158.4 (C_{trz}–Au). **2g′** ^1H (400 MHz, $CDCl_3$): δ 0.94–1.01 (m, 3H, CH_2CH_3), 1.32–1.44 (m, 2H, CH_2CH_3), 1.99–2.06 (m, 2H, NCH_2CH_2), 4.17 (s, 3H, NCH_3), 4.50 (t, 2H, $^3J_{HH}$ = 7.3 Hz, NCH_2), 7.58 (s, 1H, $C_{trz}H$) $^{13}C\{^1H\}$(101 MHz, $CDCl_3$): δ 13.4 or 13.6 (CH_2CH_3), 19.7 (CH_2CH_3), 32.4 (NCH_2CH_2), 38.8 (NCH_3), 55.4 (NCH_2), 134.7 ($C_{trz}H$), 157.7 (C_{trz}–Au) Anal. (%):Found: C, 23.66; H, 3.55; N, 11.08; Calcd for $C_7H_{13}AuClN_3$: C, 22.62; H,3.53; N,11.31.

Compound 3a. Neat MeOTf (12.5 μL, 0.11 mmol) was added to a solution of **2a** (40 mg, 0.094 mmol) in dry MeCN (2 mL), and the reaction mixture stirred protected from light for 5 min. PPh_3 (31 mg, 0.12 mmol) was added, and the reaction stirred for a further 15 min. The solvent was removed *in vacuo*, and the residue was purified by dissolving the product in CH_2Cl_2 and precipitation with pentane, followed by drying *in vacuo*. Complex **3a** was obtained as a white solid in quantitative yield (76 mg, 0.095 mmol). Crystals were grown by slow diffusion of Et_2O into a CH_2Cl_2 solution of **3a**. ^1H (400 MHz, $CDCl_3$): δ 0.88 (t, $^3J_{HH}$ = 7.3 Hz, 3H, $C(CH_2)_3CH_3$), 0.92 (t, $^3J_{HH}$ = 7.3 Hz, 3H, $N(CH_2)_3CH_3$), 1.32–1.49 (m, 4H, CH_2CH_3), 1.79–1.87 (m, 2H, $C_{Trz}CH_2CH_2$), 2.00–2.08 (m, 2H, NCH_2CH_2), 2.90 (t, $^3J_{HH}$ = 7.8 Hz, 2H, $C_{Trz}CH_2$), 4.18 (s, 3H, NCH_3), 4.46 (t, $^3J_{HH}$ = 7.3 Hz, 2H, NCH_2), 7.44–7.54 (m, 12H, $C_{Ar}H$), 7.54–7.59 (m, 3H, $C_{Ar}H$) $^{13}C\{^1H\}$(101 MHz, $CDCl_3$): δ 13.6 ($N(CH_2)_3CH_3$), 13.9 ($C_{Trz}(CH_2)_3CH_3$), 19.9 ($N(CH_2)_2CH_2$), 22.5 ($C_{Trz}(CH_2)_2CH_2$), 24.7 ($C_{Trz}CH_2$), 31.7 (CCH_2CH_2), 32.9 (NCH_2CH_2), 37.2 (NCH_3), 55.5 (NCH_2), 129.7 (d, J_{PC} = 11.0 Hz, $C_{Ar}H$), 132.1 (d, J_{PC} = 2.2 Hz, $C_{Ar}H$), 134.1 (d, J_{PC} = 14.2 Hz, $C_{Ar}H$), 149.9 ($C_{trz}C$), 172.0 (C_{trz}–Au) $^{31}P\{^1H\}$(162 MHz,$CDCl_3$): δ 39.4 (br) $^{19}F\{^1H\}$ (282 MHz, $CDCl_3$): δ −78.12 (s) HRMS (ESI+): *m*/*z* Found 654.2339 $[M - OTf]^+$ (calcd for $C_{29}H_{36}N_3PAu$, 654.2312).

Catalytic procedures

General procedure for the catalytic synthesis of oxazolines. To a solution of 4-bromobenzaldehyde (290 mg, 1.57 mmol) and trimethoxybenzene (60. mg, 0.36 mmol, internal standard) in CH_2Cl_2 (4 mL) in thick walled 5 mL vail was added methyl isocyanoacetate (130 μL, 1.43 mmol), followed by N^iPr_2Et (25 μL, 0.14 mmol), complex **2** (14 μmol), and the additive according to Table 2 (28 μmol). The vial was sealed, protected from light, and heated to 40 °C in an oil bath. Conversions and *cis*/*trans* ratios were monitored by ^1H NMR spectroscopy in $CDCl_3$ and compared to previously reported literature values.[37]

For reactions involving 1.1 mol% and 2 mol% MeOTf, a solution of MeOTf (0.265 M in dry, degassed CH_2Cl_2) was used and added before N^iPr_2Et. The volume of CH_2Cl_2 was adjusted to a total reaction volume of 4 mL.

General procedure for catalytic carbene transfer of EDA to benzene. Under a N_2 atmosphere and protected from light, anhydrous benzene (3 mL) was added to a Schlenk flask containing **2** (12 μmmol). Then EDA (53 μL, 0.44 mmol) was added and either $NaBAr^F{}_4$ (13.7 mg, 15 μmol) or the appropriate silver salt (13 μmol, see Table 3). The reaction was monitored by GC at 3–5 h and 20–24 h. After 24 h, the reaction was filtered, concentrated, and analysed by ^1H NMR spectroscopy ($CDCl_3$ solution).[30c,38] For runs with **2c**, the quantities were lower: **2a** (6.1 mg, 5.8 μmol), benzene (2 mL), EDA (25 μL, 0.21 mmol) and $NaBAr^F{}_4$ (7.6 mg, 8.6 μmol).

For experiments probing the carbene transfer to styrene, the experimental procedure was identical to that described above,[30c,39] except benzene was replaced by a mixture of CH_2Cl_2 (2 mL) and styrene (267 μL, 2.3 mmol).

Crystal structure determinations. Crystal data for **2b,f,g**, and **3a** were collected using a Rigaku (former Agilent Technologies) Oxford Diffraction SuperNova A diffractometer fitted with an Atlas detector and using monochromated Mo-K_α radiation (0.71073 Å). A complete dataset was collected, assuming that the Friedel pairs are not equivalent. The intensities were corrected for Lorentz and polarisation effects, and a numerical absorption correction based on Gaussian integration over a multifaceted crystal model was applied. The structures were solved by direct methods using SHELXS-97 and refined by full-matrix least squares fitting on F^2 for all data using SHELXL-97.[40] Hydrogen atoms were added at calculated positions and refined by using a riding model. Anisotropic thermal displacement parameters were used for all nonhydrogen atoms. Further crystallographic details are compiled in Tables S5–S8.† Crystallographic data for all four complexes have been deposited with the Cambridge Crystallographic Data Centre as supplementary publication no. CCDC 1481152 (**2b**), 1481154 (**2f**), 1481151 (**2g**), and 1481153 (**3a**).

Acknowledgements

This work was financially supported by the European Research Council (CoG 615653), the European Science Foundation (COST Action CM 1205), MINECO (CTQ2014-52769-CO3-1-R), the Junta de Andalucía (P10-FQM-06292), Ryerson University (R. A. G.), and the Irish Research Council through a fellowship to. R. P. We thank Dr D. Conseco-Gonzales for the synthesis of complex **2e**. We thank the group of Chemical Crystallography of the University of Bern (PD Dr P. Macchi) for the X-ray structure solution of **2f** and the Swiss National Science Foundation (R'equip project 206021_128724) for co-funding the single crystal X-ray diffractometer at the department of Chemistry and Biochemistry of the University of Bern.

References

1 (*a*) D. Pflästerer and A. S. K. Hashmi, *Chem. Soc. Rev.*, 2016, **45**, 1331–1367; (*b*) Z. Zheng, Z. Wang, Y. Wang and L. Zhang, *Chem. Soc. Rev.*, 2016, DOI: 10.1039/C5CS00887E; (*c*) M. Joost, A. Amgoune and D. Bourissou, *Angew. Chem., Int. Ed.*, 2015, **54**, 15022–15045; (*d*) B. Ranieri, I. Escofet and A. M. Echavarren, *Org. Biomol. Chem.*, 2015, **13**, 7103–7118; (*e*) M. Jia and M. Bandini, *ACS Catal.*, 2015, **5**, 1638–1652;

(*f*) H. G. Raubenheimer and H. Schmidbaur, *J. Chem. Educ.*, 2014, **91**, 2024–2036; (*g*) J. Xie, C. Pan, A. Abdukader and C. Zhu, *Chem. Soc. Rev.*, 2014, **43**, 5245–5256; (*h*) L. Fensterbank and M. Malacria, *Acc. Chem. Res.*, 2014, **47**, 953–965; (*i*) R. E. M. Brooner and R. A. Widenhoefer, *Angew. Chem., Int. Ed.*, 2013, **52**, 11714–11724; (*j*) H. A. Wegner and M. Auzias, *Angew. Chem., Int. Ed.*, 2011, **50**, 8236–8247; (*k*) S. P. Nolan, *Acc. Chem. Res.*, 2011, **44**, 91–100; (*l*) N. Krause and C. Winter, *Chem. Rev.*, 2011, **111**, 1994–2009; (*m*) N. Shapiro and F. Toste, *Synlett*, 2010, 675–691; (*n*) C. Nevado, *Chimia*, 2010, **64**, 247–251; (*o*) R. A. Widenhoefer, *Chem. – Eur. J.*, 2008, **14**, 5382–5391; (*p*) D. J. Gorin, B. D. Sherry and F. D. Toste, *Chem. Rev.*, 2008, **108**, 3351–3378; (*q*) A. Arcadi, *Chem. Rev.*, 2008, **108**, 3266–3325; (*r*) Z. Li, C. Brouwer and C. He, *Chem. Rev.*, 2008, **108**, 3239–3265; (*s*) A. Fürstner and P. W. Davies, *Angew. Chem., Int. Ed.*, 2007, **46**, 3410–3449.

2 (*a*) D. Gatineau, J. Goddard, V. Mouriès-Mansuy and L. Fensterbank, *Isr. J. Chem.*, 2013, **53**, 892–900; (*b*) S. Díez-González, N. Marion and S. P. Nolan, *Chem. Rev.*, 2009, **109**, 3612–3676; (*c*) H. G. Raubenheimer and S. Cronje, *Chem. Soc. Rev.*, 2008, **37**, 1998–2011. For applications of Au(NHC) complexes in other areas, see for example: (*d*) M. Baron, S. Bellemin-Laponnaz, C. Tubaro, M. Basato, S. Bogialli and A. Dolmella, *J. Inorg. Biochem.*, 2014, **141**, 94–102; (*e*) C. Bazzicalupi, M. Ferraroni, F. Papi, L. Massai, B. Bertrand, L. Messori, P. Gratteri and A. Casini, *Angew. Chem., Int. Ed.*, 2016, **55**, 4256–4259.

3 (*a*) B. Schulze and U. S. Schubert, *Chem. Soc. Rev.*, 2014, **43**, 2522–2571; (*b*) K. F. Donnelly, A. Petronilho and M. Albrecht, *Chem. Commun.*, 2013, **49**, 1145–1159; (*c*) J. D. Crowley, A.-L. Lee and K. J. Kilpin, *Aust. J. Chem.*, 2011, **64**, 1118–1132; (*d*) P. Mathew, A. Neels and M. Albrecht, *J. Am. Chem. Soc.*, 2008, **130**, 13534–13535; (*e*) G. Guisado-Barrios, J. Bouffard, B. Donnadieu and G. Bertrand, *Angew. Chem., Int. Ed.*, 2010, **49**, 4759–4762.

4 For examples, see: (*a*) D. R. Tolentino, L. Jin, M. Melaimi and G. Bertrand, *Chem. – Asian J.*, 2015, **10**, 2139–2142; (*b*) D. Mendoza-Espinosa, R. González-Olvera, G. E. Negrón-Silva, D. Angeles-Beltrán, O. R. Suárez-Castillo, A. Álvarez-Hernández and R. Santillan, *Organometallics*, 2015, **34**, 4529–4542; (*c*) D. Mendoza-Espinosa, R. González-Olvera, C. Osornio, G. E. Negrón-Silva and R. Santillan, *New J. Chem.*, 2015, **39**, 1587–1591; (*d*) C. Mejuto, G. Guisado-Barrios, D. Gusev and E. Peris, *Chem. Commun.*, 2015, **51**, 13914–13917; (*e*) L.-A. Schaper, X. Wei, S. J. Hock, A. Pöthig, K. Öfele, M. Cokoja, W. A. Herrmann and F. E. Kühn, *Organometallics*, 2013, **32**, 3376–3384; (*f*) L.-A. Schaper, K. Öfele, R. Kadyrov, B. Bechlars, M. Drees, M. Cokoja, W. A. Herrmann and F. E. Kühn, *Chem. Commun.*, 2012, **48**, 3857–3859; (*g*) K. J. Kilpin, U. S. D. Paul, A.-L. Lee and J. D. Crowley, *Chem. Commun.*, 2011, **47**, 328–330.

5 (*a*) J. E. Hein and V. V. Fokin, *Chem. Soc. Rev.*, 2010, **39**, 1302–1315; (*b*) J. E. Moses and A. D. Moorhouse, *Chem. Soc. Rev.*, 2007, **36**, 1249–1262; (*c*) V. D. Bock, H. Hiemstra and J. H. van Maarseveen, *Eur. J. Org. Chem.*, 2006, 51–68; (*d*) V. V. Rostovtsev, L. G. Green, V. V. Fokin and K. B. Sharpless, *Angew. Chem., Int. Ed.*, 2002, **41**, 2596–2599.

6 V. Leigh, W. Ghattas, R. Lalrempuia, H. Müller-Bunz, M. T. Pryce and M. Albrecht, *Inorg. Chem.*, 2013, **52**, 5395–5402.

7 (*a*) I. Corbucci, A. Petronilho, H. Müller-Bunz, L. Rocchigiani, M. Albrecht and A. Macchioni, *ACS Catal.*, 2015, **5**, 2714–2718; (*b*) C. Cesari, R. Mazzoni, H. Müller-Bunz and M. Albrecht, *J. Organomet. Chem.*, 2015, **793**, 256–262; (*c*) A. Petronilho, A. Llobet and M. Albrecht, *Inorg. Chem.*, 2014, **53**, 12896–12901; (*d*) D. Canseco-Gonzalez and M. Albrecht, *Dalton Trans.*, 2013, **42**, 7424–7432.

8 (*a*) N. Marion and S. P. Nolan, *Chem. Soc. Rev.*, 2008, **37**, 1776–1782; (*b*) I. J. Lin and C. S. Vasam, *Can. J. Chem.*, 2005, **83**, 812–825.

9 (*a*) Z. Lu, J. Han, G. B. Hammond and B. Xu, *Org. Lett.*, 2015, **17**, 4534–4537; (*b*) A. Zhdanko and M. E. Maier, *ACS Catal.*, 2014, **4**, 2770–2775; (*c*) D. Wang, R. Cai, S. Sharma, J. Jirak, S. K. Thummanapelli, N. G. Akhmedov, H. Zhang, X. Liu, J. L. Petersen and X. Shi, *J. Am. Chem. Soc.*, 2012, **134**, 9012–9019; (*d*) H. Schmidbaur and A. Schier, *Z. Naturforsch., B: Chem. Sci.*, 2011, **66**, 329–350; (*e*) S. R. Patrick, I. I. F. Boogaerts, S. Gaillard, A. M. Z. Slawin and S. P. Nolan, *Beilstein J. Org. Chem.*, 2011, **7**, 892–896; (*f*) D. Weber, M. A. Tarselli and M. R. Gagné, *Angew. Chem., Int. Ed.*, 2009, **48**, 5733–5736.

10 (*a*) L. Ricard and F. Gagosz, *Organometallics*, 2007, **26**, 4704–4707; (*b*) A. Buzas and F. Gagosz, *J. Am. Chem. Soc.*, 2006, **128**, 12614–12615; (*c*) N. Mézailles, L. Ricard and F. Gagosz, *Org. Lett.*, 2005, **7**, 4133–4136.

11 (*a*) A. Homs, C. Obradors, D. Lebœuf and A. M. Echavarren, *Adv. Synth. Catal.*, 2014, **356**, 221–228; (*b*) C. Obradors, D. Leboeuf, J. Aydin and A. M. Echavarren, *Org. Lett.*, 2013, **15**, 1576–1579; (*c*) P. R. McGonigal, C. de León, Y. Wang, A. Homs, C. R. Solorio-Alvarado and A. M. Echavarren, *Angew. Chem., Int. Ed.*, 2012, **51**, 13093–13096; (*d*) C. R. Solorio-Alvarado, Y. Wang and A. M. Echavarren, *J. Am. Chem. Soc.*, 2011, **133**, 11952–11955; (*e*) V. López-Carrillo and A. M. Echavarren, *J. Am. Chem. Soc.*, 2010, **132**, 9292–9294; (*f*) C. H. M. Amijs, V. López-Carrillo, M. Raducan, P. Pérez-Galán, C. Ferrer and A. M. Echavarren, *J. Org. Chem.*, 2008, **73**, 7721–7730.

12 (*a*) P. García-García, A. Martínez, A. M. Sanjuán, M. A. Fernández-Rodríguez and R. Sanz, *Org. Lett.*, 2011, **13**, 4970–4973; (*b*) R. Kinjo, B. Donnadieu and G. Bertrand, *Angew. Chem., Int. Ed.*, 2011, **50**, 5560–5563; (*c*) P. de Frémont, E. D. Stevens, M. R. Fructos, M. Mar Díaz-Requejo, P. J. Pérez and S. P. Nolan, *Chem. Commun.*, 2006, 2045–2047; (*d*) M. Sawamura, Y. Nakayama, T. Kato and

Y. Ito, *J. Org. Chem.*, 1995, **60**, 1727–1732; (*e*) A. Togni and S. D. Pastor, *J. Org. Chem.*, 1990, **55**, 1649–1664; (*f*) S. D. Pastor and A. Togni, *J. Am. Chem. Soc.*, 1989, **111**, 2333–2334; (*g*) Y. Ito, M. Sawamura and T. Hayashi, *J. Am. Chem. Soc.*, 1986, **108**, 6405–6406.

13 S. Gaillard, C. S. J. Cazin and S. P. Nolan, *Acc. Chem. Res.*, 2012, **45**, 778–787.

14 (*a*) S. K. Schneider, W. A. Herrmann and E. Herdtweck, *Z. Anorg. Allg. Chem.*, 2003, **629**, 2363–2370; (*b*) P. García-Domínguez and C. Nevado, *J. Am. Chem. Soc.*, 2016, **138**, 3266–3269.

15 (*a*) A. Guérinot, W. Fang, M. Sircoglou, C. Bour, S. Bezzenine-Lafollée and V. Gandon, *Angew. Chem., Int. Ed.*, 2013, **52**, 5848–5852; (*b*) W. Fang, M. Presset, A. Guérinot, C. Bour, S. Bezzenine-Lafollée and V. Gandon, *Chem. – Eur. J.*, 2014, **20**, 5439–5446.

16 (*a*) M. Wegener, F. Huber, C. Bolli, C. Jenne and S. F. Kirsch, *Chem. – Eur. J.*, 2015, **21**, 1328–1336; (*b*) R. Manzano, T. Wurm, F. Rominger and A. S. K. Hashmi, *Chem. – Eur. J.*, 2014, **20**, 6844–6848; (*c*) M. J. López-Gómez, D. Martin and G. Bertrand, *Chem. Commun.*, 2013, **49**, 4483–4485; (*d*) K. Ji, Y. Zhao and L. Zhang, *Angew. Chem., Int. Ed.*, 2013, **52**, 6508–6512; (*e*) Y. Luo, K. Ji, Y. Li and L. Zhang, *J. Am. Chem. Soc.*, 2012, **134**, 17412–17415; (*f*) X. Zeng, M. Soleilhavoup and G. Bertrand, *Org. Lett.*, 2009, **11**, 3166–3169.

17 (*a*) J. Serra, C. J. Whiteoak, F. Acuña-Parés, M. Font, J. M. Luis, J. Lloret-Fillol and X. Ribas, *J. Am. Chem. Soc.*, 2015, **137**, 13389–13397; (*b*) S. Bastin, C. Barthes, N. Lugan, G. Lavigne and V. César, *Eur. J. Inorg. Chem.*, 2015, 2216–2221.

18 D. Canseco-Gonzalez, A. Petronilho, H. Mueller-Bunz, K. Ohmatsu, T. Ooi and M. Albrecht, *J. Am. Chem. Soc.*, 2013, **135**, 13193–13203.

19 J. R. Wright, P. C. Young, N. T. Lucas, A. Lee and J. D. Crowley, *Organometallics*, 2013, **32**, 7065–7076.

20 L. Hettmanczyk, S. Manck, C. Hoyer, S. Hohloch and B. Sarkar, *Chem. Commun.*, 2015, **51**, 10949–10952.

21 (*a*) J. Turek, I. Panov, P. Švec, Z. Růžičková and A. Růžička, *Dalton Trans.*, 2014, **43**, 15465–15474; (*b*) H. Schmidbaur and A. Schier, *Chem. Soc. Rev.*, 2012, **41**, 370–412; (*c*) S. Guo, J. C. Bernhammer and H. V. Huynh, *Dalton Trans.*, 2015, **44**, 15157–15165.

22 D. Weber and M. R. Gagné, *Org. Lett.*, 2009, **11**, 4962–4965.

23 It has also been postulated that the reverse ligand transfer leads to a slow release of cationic Au(I) species which are underligated, and therefore potentially catalytically highly active, see ref. 15.

24 D. M. Gove, G. van Koten, J. N. Louwen, J. G. Noltes, A. L. Spek and H. J. C. Ubbels, *J. Am. Chem. Soc.*, 1982, **104**, 6609–6616.

25 M. T. Johnson, J. Marthinus Janse van Rensburg, M. Axelsson, M. S. G. Ahlquist and O. F. Wendt, *Chem. Sci.*, 2011, **2**, 2373–2377.

26 M. V. Baker, P. J. Barnard, S. J. Berners-Price, S. K. Brayshaw, J. L. Hickey, B. W. Skelton and A. H. White, *J. Organomet. Chem.*, 2005, **690**, 5625–5635.

27 (*a*) V. A. Soloshonok, A. D. Kacharov, D. V. Avilov, K. Ishikawa, N. Nagashima and T. Hayashi, *J. Org. Chem.*, 1997, **62**, 3470–3479; (*b*) A. V. Gulevich, A. G. Zhdanko, R. V. A. Orru and V. G. Nenajdenko, *Chem. Rev.*, 2010, **110**, 5235–5331; (*c*) C. Hubbert and A. S. K. Hashmi, in *Modern Gold Catalyzed Synthesis*, ed. A. S. K. Hashmi and F. D. Toste, Wiley-VCH, Weinheim, Germany, 2012, pp. 237–261.

28 The potassium salts on their own and in the absence of complex **2a** reach only medicore conversion (entry 2). When using 5% potassium salt instead of the 2% as in runs containing **2a**, a maximum of 20% conversion was observed after 8 h, see also Table S1.†

29 R. Heath, H. Müller-Bunz and M. Albrecht, *Chem. Commun.*, 2015, **51**, 8699–8701.

30 (*a*) M. M. Díaz-Requejo and P. J. Pérez, *Chem. Rev.*, 2008, **108**, 3379–3394; (*b*) M. M. Díaz-Requejo and P. J. Pérez, *J. Organomet. Chem.*, 2005, **690**, 5441–5450; (*c*) M. R. Fructos, T. R. Belderrain, P. de Frémont, N. M. Scott, S. P. Nolan, M. M. Díaz-Requejo and P. J. Pérez, *Angew. Chem., Int. Ed.*, 2005, **44**, 5284–5288; (*d*) M. Delgado-Rebollo, Á. Beltrán, A. Prieto, M. Mar Díaz-Requejo, A. M. Echavarren and P. J. Pérez, *Eur. J. Inorg. Chem.*, 2012, 1380–1386; (*e*) A. Prieto, M. R. Fructos, M. Mar Díaz-Requejo, P. J. Pérez, P. Pérez-Galán, N. Delpont and A. M. Echavarren, *Tetrahedron*, 2009, **65**, 1790–1793.

31 A. Caballero, M. M. Díaz-Requejo, M. R. Fructos, A. Olmos, J. Urbano and P. J. Pérez, *Dalton Trans.*, 2015, **44**, 20295–20307.

32 (*a*) R. Gava, A. Olmos, B. Noverges, T. Varea, E. Álvarez, T. R. Belderrain, A. Caballero, G. Asensio and P. J. Pérez, *ACS Catal.*, 2015, **5**, 3726–3730; (*b*) M. R. Fructos, T. R. Belderrain, M. C. Nicasio, S. P. Nolan, H. Kaur, M. M. Díaz-Requejo and P. J. Pérez, *J. Am. Chem. Soc.*, 2004, **126**, 10846–10847.

33 Y. Xi, Y. Su, Z. Yu, B. Dong, E. J. McClain, Y. Lan and X. Shi, *Angew. Chem., Int. Ed.*, 2014, **53**, 9817–9821.

34 (*a*) Y. Wang, M. E. Muratore and A. M. Echavarren, *Chem. – Eur. J.*, 2015, **21**, 7332–7339; (*b*) D. Benitez, N. D. Shapiro, E. Tkatchouk, Y. Wang, W. A. Goddard and F. D. Toste, *Nat. Chem.*, 2009, **1**, 482–486; (*c*) A. M. Echavarren, *Nat. Chem.*, 2009, **1**, 431–433; (*d*) A. S. K. Hashmi, *Angew. Chem., Int. Ed.*, 2008, **47**, 6754–6756.

35 R. W. Read and X. B. Wang, *Chiang Mai J. Sci.*, 2009, **36**, 247–257.

36 (*a*) A. Poulain, D. Canseco-Gonzalez, R. Hynes-Roche, H. Müller-Bunz, O. Schuster, H. Stoeckli-Evans, A. Neels and M. Albrecht, *Organometallics*, 2011, **30**, 1021–1029; (*b*) S. S. Khan, S. Hanelt and J. Liebscher, *ARKIVOC*, 2009, **xii**, 193–208.

37 H. Ohta, Y. Uozumi and Y. M. A. Yamada, *Chem. – Asian J.*, 2011, **6**, 2545–2549.

38 (*a*) W. D. Mackay and J. S. Johnson, *Org. Lett.*, 2016, **18**, 536–539; (*b*) N. Komine, J. A. Flores, K. Pal, K. G. Caulton and D. J. Mindiola, *Organometallics*, 2013, **32**, 3185–3191;

(*c*) A. K. Padala, V. Saikam, A. Ali and Q. N. Ahmed, *Tetrahedron*, 2015, **71**, 9388–9395.

39 (*a*) J. S. Yadav, B. V. S. Reddy and P. N. Reddy, *Adv. Synth. Catal.*, 2004, **346**, 53–56; (*b*) D. A. Evans, K. A. Woerpel, M. M. Hinman and M. M. Faul, *J. Am. Chem. Soc.*, 1991, **113**, 726–728.

40 G. M. Sheldrick, *Acta Crystallogr., Sect. A: Fundam. Crystallogr.*, 2008, **64**, 112.